Theoretical modelling of the self-tapping screw fastening process

L D Seneviratne*, F A Ngemoh, S W E Earles and **K A Althoefer**
Department of Mechanical Engineering, King's College London, UK

Abstract: The results of a theoretical study of the self-tapping screw insertion process are presented. Fundamental concepts of engineering mechanics are employed to analyse the axial torque required to complete a general self-tapping screw insertion operation. Equations for the screw insertion torque as a function of screw, hole and material properties are presented. Experimental results for torque signature signals are compared with the predictions of the theoretical model, confirming the validity of the model. The theoretical model provides a basis for developing automated monitoring and control strategies for self-tapping screw fastenings.

Keywords: screw insertions, automated assembly, torque signature signals, fault diagnosis, monitoring

NOTATION

A_c	screw thread cross-sectional area
A_e	contact area of the screw during engagement on the lateral cross-sectional plane
A_f	surface area of the engaged screw thread (relating to friction)
A_h	effective contact area of the screw cap plane
A_z	section area of the screw thread lying on the surface of the screw mean diameter cylinder
C_1	first point on the screw at which contact is made with the hole
C_2	first point of maximum diameter on the screw from the tip (end of screw taper)
$\mathbf{C}_f$	transformation matrix from the coordinate system $[\boldsymbol{n}, \boldsymbol{t}, \boldsymbol{z}]$ to $[\boldsymbol{x}, \boldsymbol{y}, \boldsymbol{z}]$
d	combined deflection of the screw and formed threads
d_1	deflection of the formed threads
d_2	deflection of the screw threads
D_h	tap-hole diameter
D_r	root diameter of the screw
D_{re}	effective screw root diameter (root diameter for full threads on the screw)
D_s	major diameter of the screw
D_{sh}	screw head diameter
e	direct strain
E	elastic modulus
F_e	engagement axial force
F_{fi}, F_{fj}, F_{fk}	components of the friction and normal forces on the screw thread along the coordinate axes i, j, k
F_N	normal force on the screw thread surface
F_{Nl}	normal force on the lower surface of the screw thread
F_{NO}	normal force on the screw thread surface resulting from interface pressure
F_{Nu}	normal force on the upper surface of the screw thread
F_s	force magnitude relating to cutting shear resistance
$\boldsymbol{F}_s$	force vector relating to cutting shear resistance
F_{tb}	reaction force component on the screw thread owing to contact forces on the screw cap
F_{th}	contact force between the screw cap and the sandwich plate
h	height of the screw thread from root to crest
$[i, j, k]$	components of force, moment or acceleration in $[\boldsymbol{x}, \boldsymbol{y}, \boldsymbol{z}]$

The MS was received on 13 December 1999 and was accepted after revision for publication on 7 April 2000.
** Corresponding author: Department of Mechanical Engineering, King's College London, Strand, London WC2R 2LS, UK.*

$K_f(\phi)$	geometric parameter relating to friction forces
K_{th}	stiffness coefficient of the joint under compression
l	length of the screw thread along the helix
L_s	effective length of the screw along its central axis
M_{fi}, M_{fj}, M_{fk}	moment components against friction resistance about the respective axes
M_{si}, M_{sj}, M_{sk}	moment components against shear resistance about the respective axes
$[n, t, z]$	components of force, moment or acceleration in $[\boldsymbol{n}, \boldsymbol{t}, \boldsymbol{z}]$
p	screw pitch
P	arbitrary point on the hole wall
P_1	mid-point on the screw thread cross-sectional plane
P_2	centroid of the screw thread cross-sectional area
r_f	radial distance to the mid-point of the screw thread cross-sectional area (friction forces)
r_s	radial distance to the centroid of the screw thread cross-sectional area (cutting forces)
$\boldsymbol{R}_s$	position vector to the point of action of shear forces
t_1	thickness of the near (sandwich) plate
t_2	thickness of the tap plate
T_e	engagement torque
T_{fz}	torque required about the screw central axis against driving friction resistance
T_{sz}	torque component required about the screw central axis against shear (cutting) resistance
w	width of the screw thread triangle from root to crest
$[\boldsymbol{x}, \boldsymbol{y}, \boldsymbol{z}]$, $[\boldsymbol{n}, \boldsymbol{t}, \boldsymbol{z}]$	coordinate system variables as defined in Fig. 3
z_{em}	mean axial distance of the engaged threads
α	angular position value corresponding to the length of the screw cutting portion
β	screw thread crest half-angle
γ	ratio of screw engagement rotation angle to taper rotation angle
δ	elemental value
Δt	axial compression in the joint
$\Delta\phi$	angular displacement increment from the beginning of final tightening
ζ	discontinuous function correcting for the partly engaging screw taper
θ	thread helix angle
θ_e	effective helix angle during engagement when rotation is independent of axial translation
μ	friction coefficient at the screw/hole thread interface
μ_h	friction coefficient at the screw cap interface
σ	direct stress
σ_1	stress set-up during engagement on contact area A_e in the axial direction
σ_2	stress set-up during engagement on contact area A_f in the tangential direction
σ_{max}	maximum direct stress
σ_{uts}	ultimate tensile stress of the tap-plate material
σ_y	yield stress
σ_z	compressive stress resulting from contact of the screw cap with the near plate
τ	shear stress
τ_{max}	maximum shear stress
ϕ	helix coordinate variable
ϕ_b	angular position corresponding to screw breakthrough
ϕ_t	angular position corresponding to the beginning of final tightening
Φ	angular displacement with rotation independent of axial translation
Φ'	angular velocity with rotation independent of axial translation
ψ	discontinuous function correcting for the partly breaking through screw taper

1 INTRODUCTION

Screw fastening is a popular assembly method accounting for over a quarter of all assembly operations [1]. Parts fastened together by means of screws can be disassembled for repair and maintenance and subsequently reassembled. Another advantage is that the parts can be clamped together with varying degrees of compressive force by controlling the final tightening torque.

The integrity of a threaded joint depends on the tightening torque, the travel of the screw and the quality of the screw and hole. Power tools are now frequently employed to increase the speed of screw insertions. Typically, human operators or robotic devices position and orientate the screw relative to the workpiece before the power tool turns and tightens the screw. However, the speed of this operation reduces the operator's monitoring and error recovery response time, resulting in increased rejects.

Automating the screw insertion task using control and monitoring strategies is attractive to manufacturers. The main controlled parameter in automated screw fastening

strategies is the axial torque applied by the tool to the screw head. Typically, current commercially available screw insertion power tools control the final tightening torque using a mechanical clutch, which disengages once a preset torque level is reached. They are open-loop control devices with no monitoring capabilities.

Even though there has been a growing research interest in the field of assembly automation since the early 1970s, particularly in relation to the simple peg-in-hole insertion problem, there has been little published material on the screw insertion task. In 1978, Nevins and Whitney [**1**] presented the results of research into different types of subassembly tasks required to assemble a range of common products, catalogued by Kondoleon [**2**]. From this investigation, screw fastenings were shown to account for about 27 per cent of the assembly tasks, second only to simple-peg-in-hole fastenings which accounted for about 33 per cent. Hence, automating the screw insertion task has been identified as desirable in a number of industries, particularly those involved in the manufacture of domestic products.

In 1980, Smith [**3**] provided an overview of the automatic screwdriver technology then in use and proposed various strategies for the control and monitoring of the screw insertion process. The screwdriver was fitted with a torque sensor and an optical encoder in order to produce a signature signal during fastenings. This signature signal was then used for assessing the quality of the fastening.

In 1982, Ogiso and Watanabe [**4**] experimentally investigated the influence of position error between the driver bit and the threaded holes, concluding that, in general, a positioning accuracy of better than 0.5 mm is required for reliable operation. In 1993, Nicolson and Fearing [**5**] presented a screw insertion model, analysing the geometric constraints during threaded fastenings. They investigated the influence of errors in the angle of tilt (orientation errors) and derived expressions for minimum tilt angle error in order to avoid cross-threading and jamming.

The main motivation for this study is the desire to develop automated monitoring and feedback control strategies for small electric-powered screwdrivers (SEPS). This requires a model of a typical screw insertion process. The model may be considered as a single-input–single-output process, where the torque is the input and the resulting screw displacement the output. Recently, the results of an experimental investigation on torque signature signals were presented [**6**]. However, an accurate theoretical model to predict torque signature signals is required.

This study theoretically investigates the nature of torque–displacement curves for a general self-tapping screw fastening operation. Fundamental concepts of engineering mechanics are employed to analyse the forces required to complete a general self-tapping screw insertion operation. Equations for screw insertion torque as a function of screw, hole and material properties are presented. Experimental results for torque signature signals are compared with the predictions of the theoretical model, confirming the validity of the model. The theoretical model provides a basis for developing automated monitoring and control strategies for self-tapping screw fastenings.

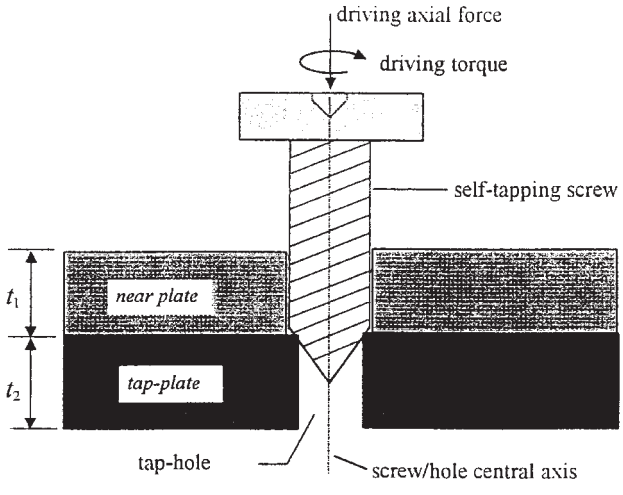

Fig. 1 General self-tapping screw insertion

2 PROBLEM DEFINITION

An idealized self-tapping screw insertion operation is considered. The task involves fastening together two plates using a self-tapping screw, driven by a torque about the screw central axis and a force along its central axis. The two plates, referred to as the near plate and the tap plate (Fig. 1) are rigidly held together. The near plate has a thickness of t_1 and a clearance hole through which the screw moves freely. The tap plate has a thickness of t_2 and a hole to be threaded by the screw, referred to as the tap hole.

2.1 Screw geometry

The screw is modelled as a helical thread with a triangular section. The generalized self-tapping screw geometry is shown in Fig. 2a, consisting of the body, the screw thread and the screw head. The bulk of the screw body is cylindrical in shape and is tapered at the free end. The screw head is considered circular with a flat lower flange having an effective diameter, D_{sh}, and lying on a plane normal to the screw central axis. The screw body has a root diameter, D_r, measured at the root of the screw thread and a major diameter, D_s, measured at the crest of the screw thread. The effective length of the screw body, L_s, is the distance along the screw axis from

the lower flange of the screw head to the point on the screw taper where the screw diameter is equal to the tap-hole diameter.

The screw thread is helical and wound round the entire length of the screw body (from the screw tip to the point where the screw body meets the lower flange of the screw head), at a helical angle of θ and a pitch of p. The unwound geometry of the screw thread (Fig. 2b) has an overall length l. It has a triangular cross-section (Fig. 2c) with sides of width w and inclined at an angle β to the normal drawn from the screw cylinder. The height of the thread from crest to root is h. The centre and the centroid of the triangle are at P_1 and P_2 respectively.

2.2 Ideal screw fastening conditions

The following conditions are assumed true for the idealized case considered in this study:

1. The near plate has a clearance hole with a diameter

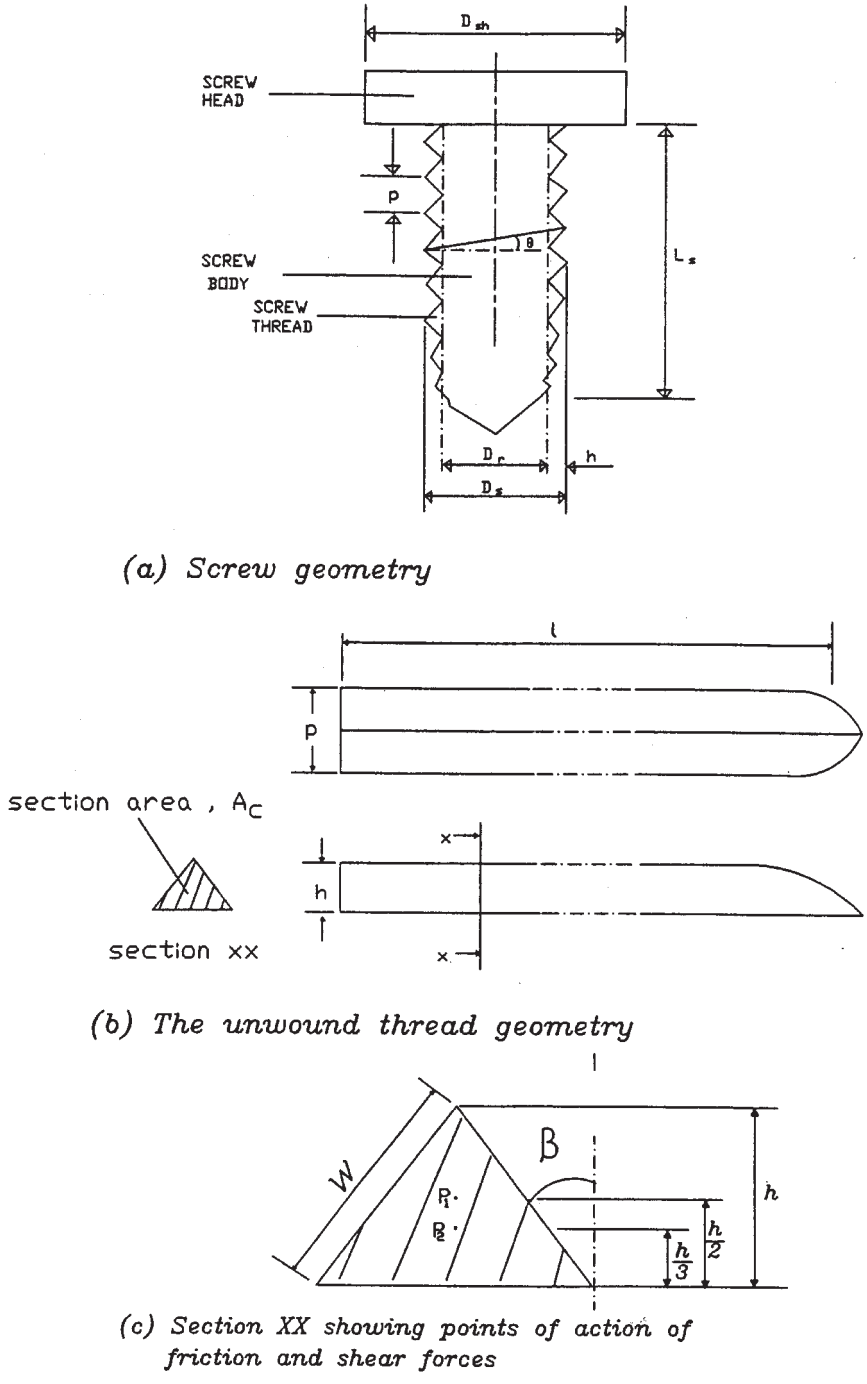

Fig. 2 Screw and thread geometry

greater than the screw major diameter and a flat surface plane normal to the hole central axis.
2. The tap plate has a clean hole with diameter D_h, where $D_h \geqslant D_r$.
3. The holes on the near and tap plates are perfectly aligned on a single central axis and the components are rigidly held together.
4. The screw is rigidly held by the driver, and no rotation or translation is permitted except about and along the screw central axis.
5. The screw is centrally positioned and correctly orientated in the holes.
6. The driver applies just sufficient axial force and torque to allow the screw to advance.

The forces acting on the screw are examined as it is driven from first engagement in the tap plate to final tightening, making use of fundamental concepts of engineering mechanics. The analysis considers quasi-static conditions, and force equilibrium equations are derived for each stage of the task. The screwdriver stem is assumed sufficiently rigid to counteract lateral forces. The axial torque is the main input to the process, and the axial displacement of the screw is the output of the process. It is noted that the axial force can also be considered as an input variable to the process. However, in general, screw fastening strategies do not actively control axial force, but provide a sufficient axial force to prevent slip between the tool and the screw. In this study, the axial torque is considered to be the main input variable, and it is assumed that an axial force sufficient to balance reaction forces is applied to the screw. The main objective of this analysis is to derive the input–output relationship for the self-tapping screw insertion process.

In addition to the ideal screw insertion conditions outlined above, certain other assumptions are made to reduce the complexity of the problem:

1. The tightening speeds are sufficiently low for the inertia forces to be small and negligible.
2. The plate material is homogeneous and isotropic.
3. Heat generated during screw fastenings is small and its influence on material properties is negligible.
4. The tap-hole diameter is equal to the root diameter of the screw.
5. The screw tapers uniformly from the leading end so that $dA_c/d\phi$ is constant, where A_c is the *full thread* cross-sectional area and ϕ is the helix angular position.
6. A balanced axial force is applied during screw fastening.

2.3 Coordinate systems

The coordinate systems used and the force convention adopted in this study are shown in Fig. 3. The fixed Cartesian coordinate system $[x, y, z]$ has its origin at O, the top centre of the tap hole (Fig. 3a). The helical coordinate system $[R, \phi, z]$ also has its origin at O (Fig. 3b).

A further Cartesian coordinate system, with identical orientation to the fixed frame and origin at the top centre of the top of the screw head is used to define the forces and moments acting on the screw (Fig. 3d). When the screw is fastened, two main tasks are performed:

1. *Advance screw*. Adequate forces are applied to cause a helical groove to be formed in the tap-hole wall by the advancing screw thread.
2. *Tighten screw*. Tightening forces are applied when the screw head makes contact with the near plate.

Analytical expressions for the axial torque required to perform the above tasks are derived in Sections 3 to 5.

3 AXIAL TORQUE REQUIRED TO ADVANCE SCREW

To advance the screw through the hole, two tasks have to be performed:

(a) displace material from the hole walls to create a helical groove and
(b) overcome frictional forces between the groove and the screw thread.

3.1 Torque required to displace material

A helical groove to accommodate the screw thread needs to be produced around the hole walls (Fig. 4). This is achieved, depending on screw type and material properties of the plate, by the physical removal of material from the hole walls or by plastic deformation of the hole walls along the helical path. The generation of the groove at any arbitrary point, P, on the hole wall will commence when the screw thread first contacts P, and cutting will continue until the groove cross-sectional area at P is equal to A_c, the maximum thread cross-sectional area. Let the point on the screw where cutting at P commences be C_1 and where it stops be C_2. The portion of the screw thread from C_1 to C_2 is fixed for any screw and hole size combination. This portion lies on the screw taper and will be referred to as the *cutting portion* of the screw thread. The analysis is given in Appendix 1, resulting in

$$T_{sz} = \frac{1}{\alpha} r_s A_c \sigma_{uts} [\psi(\phi, \alpha) - \zeta(\phi, \alpha)] \cos \theta \tag{10}$$

3.2 Torque required to overcome friction

Once the screw is in the hole, the engaged threads are in contact with the groove wall. The material around the

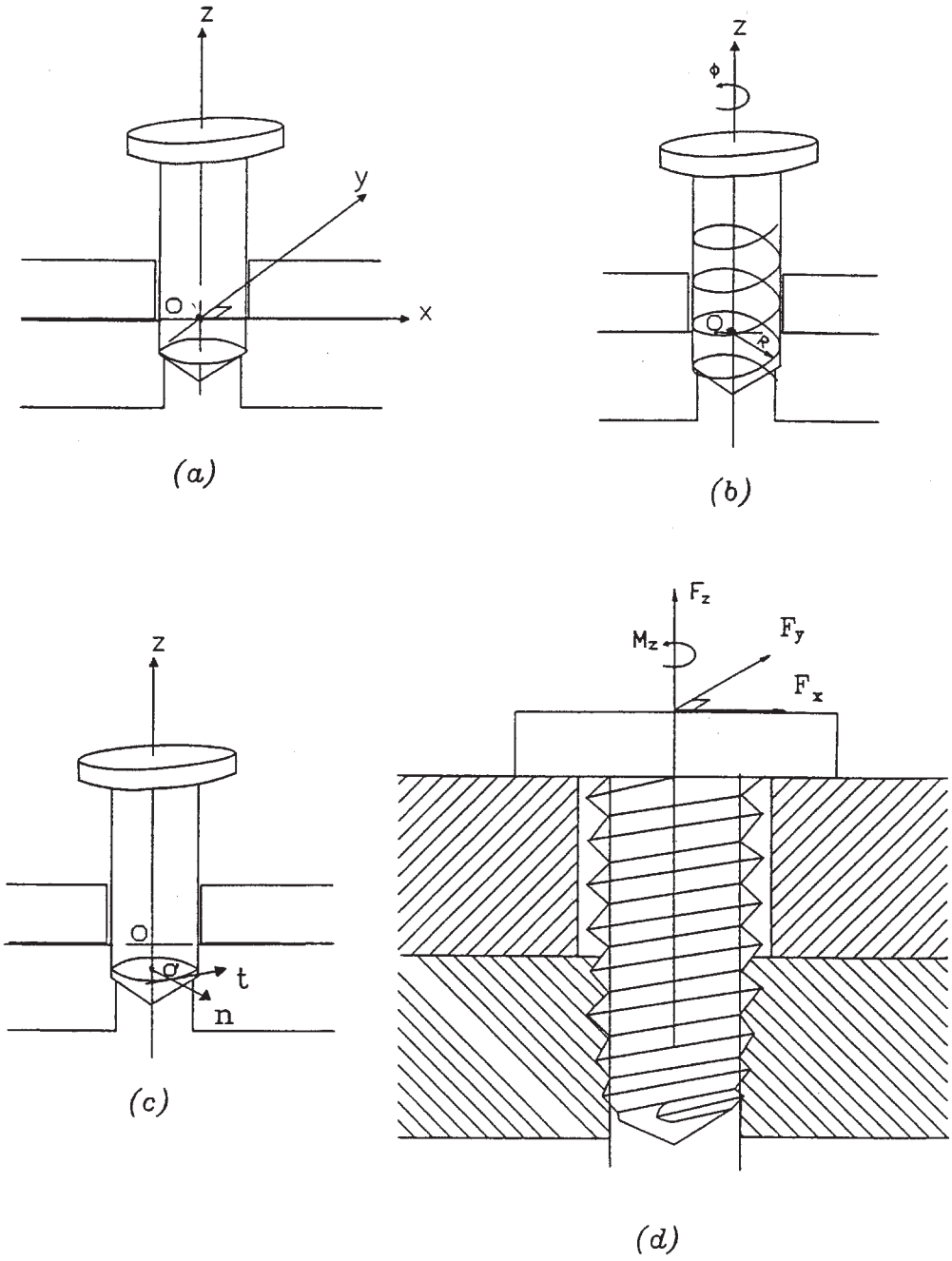

Fig. 3 Coordinate systems and force convention

groove is compressed outwards by the forces on the cutting portion of the screw thread. The tendency is therefore for the groove wall to squeeze back on to the surface of the engaged threads as the cutting portion advances. The magnitude of this pressure on the thread surface is equal to the compressive stress, σ_f, in the material, resulting from the elastic strain on the groove wall. As the screw advances, the thread surface slides against the groove surface. Consequently, friction forces result, in opposition to this relative motion. The analysis is given in Appendix 2, resulting in

$$T_{fz} = 2\mu r_f K_{f0}\sigma_f \cos\theta \min\left[\left(\phi - \frac{\alpha}{2}\right), \phi_b\right] \tag{26}$$

The above analysis considers a screw thread whose motion is already along a helical path, and which is cutting a groove on the hole wall complementary to its own helical thread. However, this state of motion does

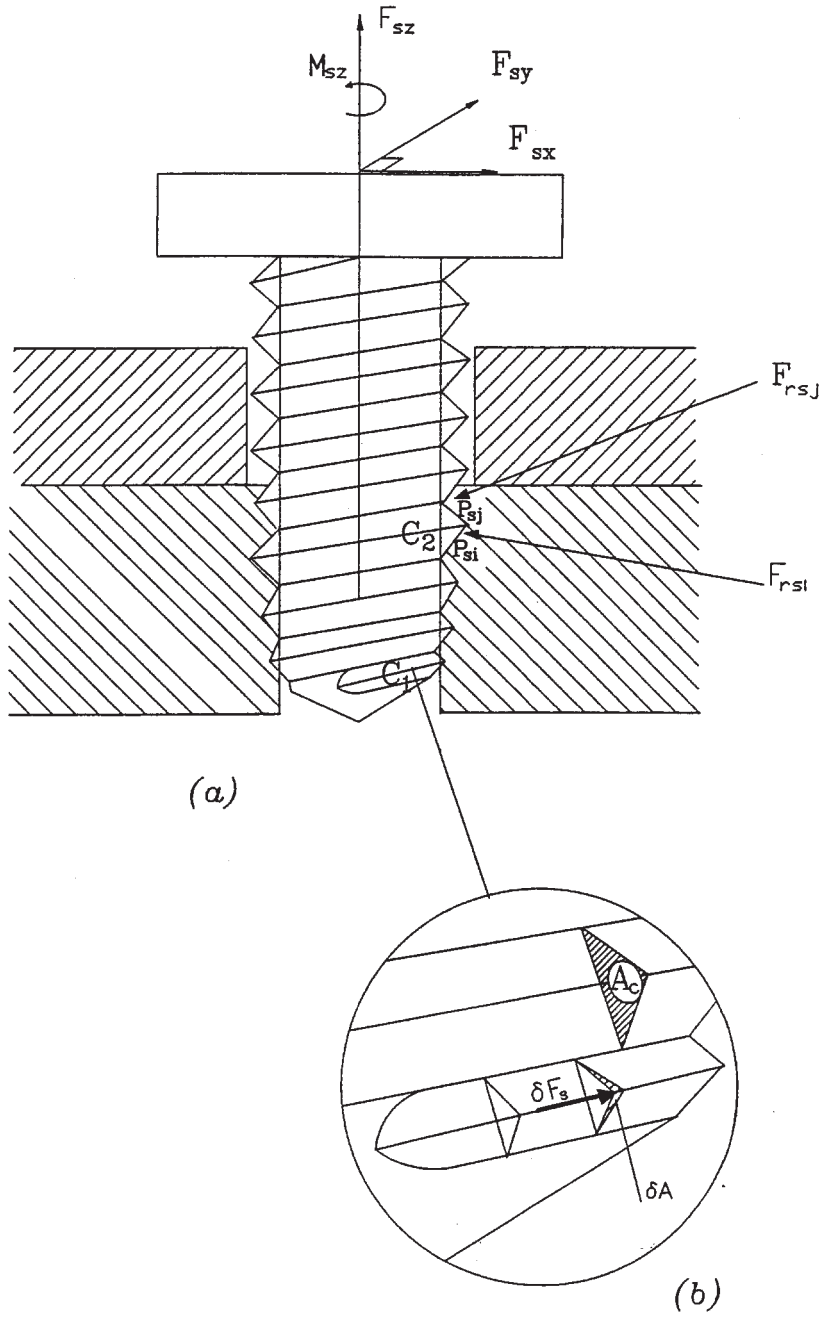

Fig. 4 Cutting force equilibrium

not start instantaneously. In order to understand the transition from free motion of the screw to thread formation in the hole, the screw engagement stage needs to be examined.

4 TORQUE REQUIRED TO ENGAGE THE SCREW

At the start of insertion, the screw is advanced along the hole central axis and contact is first made by the lower end of the cutting portion of the screw, on the upper edge of the tap-hole wall. As the screw advances, the increasing outer diameter of the cutting portion of the thread sets up compressive and shear stresses in the material. Initially, these stresses are small and the screw rotates in the hole. The screw thread in contact with the hole wall at this point slides over the wall material, elastically deforming the hole wall at the points of contact and working against the resulting friction forces on the contacting surfaces. Let two coordinate variables, z (axial position) and Φ (angular position about the

screw/hole central axis) define the position of an element of the screw thread.

The analysis is given in Appendix 3, resulting in

$$T_e = r_e \cos\left(\frac{p}{2\pi r_e}\right)\sigma_y\left(\frac{A_c}{\alpha}\phi_e + \frac{\mu K_{f0}}{\alpha}\phi_e^2\right) \quad (37)$$

The screw is considered engaged when it has turned through a complete revolution with $dz/d\Phi = p$, that is, $\phi_e = 2\pi$.

For a screw with a taper, the initial force requirements may be satisfied with relatively small values of torque, since α (proportional to the taper length) is usually larger than ϕ_e. However, for the screw threads to continue in the helical path, the torque must increase steadily to satisfy the equilibrium requirements of the screw advance stage, as presented in Section 3. At the interface, equation (37) equates to the corresponding equation presented in Section 3.

5 TORQUE REQUIRED TO TIGHTEN THE SCREW

The analyses in Sections 3 and 4 cover the state of the screw as the thread makes its way through the hole in the tap plate. At some point during this thread advance, the lower surface of the screw head makes contact with the surface of the near plate (Fig. 5). Let the helix coordinate position at this point be ϕ_t. Further increase in ϕ beyond ϕ_t will cause compression of any material of the workpiece sandwiched between the engaged threads and the screw head, as the screw cap pushes on to the near plate. The additional set of forces required to drive the screw as a result of this contact constitute the tightening components of the driving forces. In this study, the analysis is carried out assuming a balanced axial force.

The analysis is given in Appendix 4, resulting in

$$T_{tz} = \mu_h K_{th}\left[\frac{D_{sh}^3 - D_s^3}{3(D_{sh}^2 - D_s^2)}\right]\left(\frac{p\Delta\phi}{2\pi}\right) \quad (48)$$

where T_{tz} is the axial torque required to tighten the screw, as a function of the screw rotation increment, to counter the resistance to the screw motion as a result of contact of the screw cap on the near-plate surface.

6 PREDICTIONS OF THE THEORETICAL MODEL

6.1 Summary of the theoretical model

The analyses presented for the ideal self-tapping screw insertion reveal the dependence of the insertion torque on various parameters of the screw, hole and plate material. The success of the operation depends on providing the appropriate driving torque to engage the screw, drive it forward through the tap hole and finally tighten it to produce adequate clamping forces within the joint. To meet these requirements, the driver needs to generate the following axial torques:

1. *Engaging the screw*. The screw is moved to make contact with the tap hole. The axial torque, T_e, is given by equation (37). This torque is applied until the engagement condition $dz/d\Phi = p$ is satisfied. The torque depends on the screw dimensions, the yield strength of the tap-plate material, frictional resistance, screw geometry and the taper length of the screw.
2. *Advancing the screw*. The driver torque must progressively increase to counter the increasing shear force on the cutting portion of the screw thread, and the increasing friction on the engaged screw–groove thread interface. The torque required against shear resistance is given by equation (10), and the torque required against frictional resistance

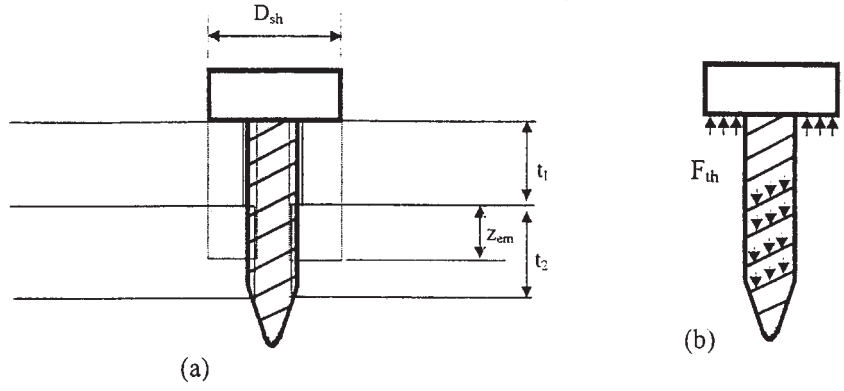

Fig. 5 Tightening forces on screw: (a) screw head makes contact with the surface of the near plate; (b) reaction force set-up on screw cap and engaged threads

is given by equation (26). Under the combined shear and friction forces, the axial torque required is given by $T_z = T_{sz} + T_{fz}$, i.e. equation (10) plus equation (26).

3. *Final tightening.* With a balanced axial force applied to the screw, the expression for the axial torque during the tightening phase is given by equation (48).

6.2 Computer simulation predictions

Equations (10), (26), (37) and (48) give the axial torque for the stages of a general self-tapping screw insertion process. These equations are employed to study the self-tapping screw fastening process, using computer simulations. The results for two tests, using ABS plastic and polycarbonate for the plate material, are given below.

As input, the equations require the screw, hole and plate material parameters listed in Tables 1 and 2. The model can then be used to predict the curve for the insertion torque versus axial displacement of the screw.

6.2.1 *Test 1—Results for ABS (PB)*

Table 1 shows the mechanical and material properties for a screw insertion using an ABS plate of 4.46 mm thickness and a self-tapping screw AB 6. The material properties were experimentally determined and the coefficient of friction was determined using an inclined plane test.

Figure 6 shows the theoretical insertion torque profile for the data in Table 1. It can be seen that the curve consists of five piecewise linear parts, corresponding to the following stages of the screw fastening:

(a) screw engagement,
(b) screw advance with thread formation,
(c) screw breakthrough,
(d) screw advance without thread formation and

Table 1 Parameters for test 1 (ABS)

Material and hole properties		Screw properties	
Material type	ABS	Type	AB 6
Thickness	4.46 mm	Material	Zinc-plated steel
Yield strength	45 MPa	Major diameter	3.42 mm
Tensile strength	45 MPa (51.1 MPa)	Root diameter	2.49 mm
Elastic modulus	2.35 GPa	Pitch	1.19 mm
Coefficient of friction	0.24 (inclined plane)	Length	9.67 mm
Tap-hole diameter	2.5 mm	Taper length	2.94 mm
Near-plate thickness	0 (not used)	Cap diameter	6.52 mm

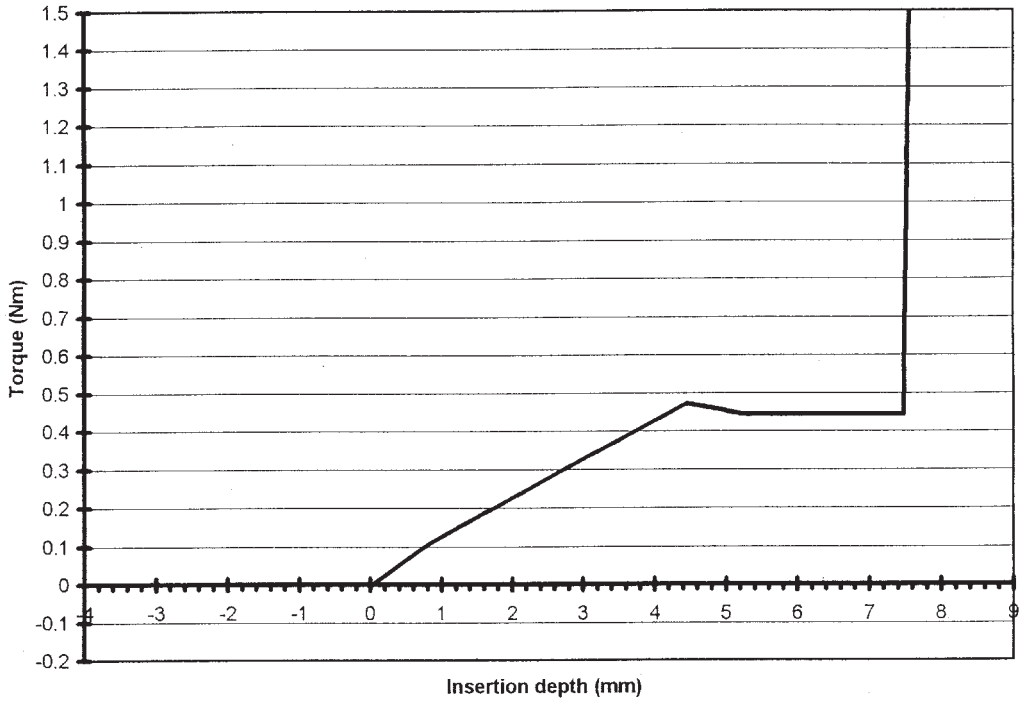

Fig. 6 Theoretical torque profile for test 1

(e) screw tightening.

The first stage begins when the tapered part of the screw makes contact with the hole and ends when the untapered part of the screw first contacts the hole. The second stage ends when the tapered part breaks through the lower part of the hole, the third stage when the untapered part of the screw breaks through the lower plate, and the fourth stage when the screw head makes first contact with the upper plate. Stage five then begins and ends when screw tightening is completed. Thus stages 1 to 4 deal with screw advancement, and stage 5 with tightening. Furthermore, stages 1 to 3 deal with combined thread cutting and overcoming friction, while stage 4 deals essentially with overcoming friction.

6.2.2 Test 2—Results for polycarbonate (PC)

Table 2 shows the mechanical and material properties for a screw insertion using a polycarbonate plate of 3 mm thickness and a self-tapping screw AB 4. The material properties in Table 2 are experimentally determined.

Figure 7 shows the theoretical insertion torque profile for the data in Table 2. In general, the shape of the torque profiles is as for the previous test, but the drop in torque from the peak value is more substantial than for ABS, reflecting the higher ultimate tensile strength against the smaller plate thickness. It is noted from the above tests that the theoretical model can be used to generate torque signature signals with relative ease, once the screw, hole and plate material parameters are known.

7 EXPERIMENTAL VALIDATION

The results from a detailed experimental study of the self-tapping screw fastening process were recently reported. Some experimental results from this study are used to validate the theoretical model. The experimental

Table 2 Parameters for test 2 (polycarbonate)

Material and hole properties		Screw properties	
Material type	Polycarbonate	Type	AB 4
Thickness	3 mm	Material	Zinc-plated steel
Yield strength	60 MPa	Major diameter	2.87 mm
Tensile strength	65.5 MPa (137.6 MPa)	Root diameter	2.02 mm
Elastic modulus	2.3 GPa	Pitch	1.10 mm
Coefficient of friction	0.19 (inclined plane)	Length	9.69 mm
Tap-hole diameter	2 mm	Taper length	2.79 mm
Near-plate thickness	0 (not used)	Cap diameter	5.03 mm

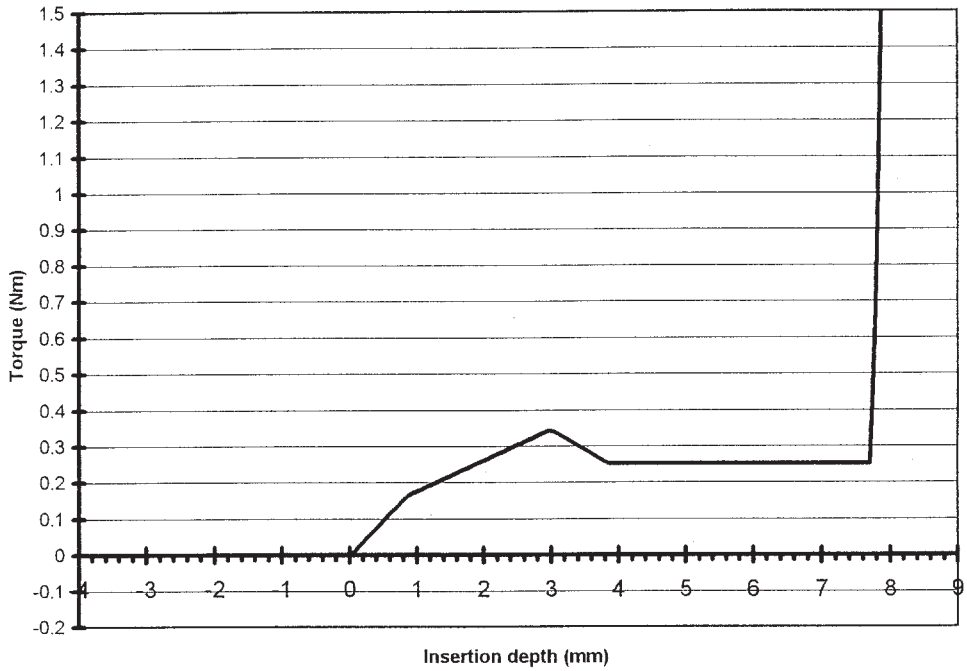

Fig. 7 Theoretical torque profile for test 2

rig consisted of a commercial autofeed screwdriver, a rotary torque transducer, a multiaxis force–torque transducer, a linear position transducer, a two-axis linear positioning table and a computer-based data acquisition and control system.

7.1 Experiment 1—Experimental results for ABS (PB)

Four experimental curves for the ABS plate are shown in Figs 8a and b, indicating a similar shape profile to the theoretical predictions. In Fig. 8, the torque rises steadily from the point of first contact (at 14.20 mm) to a peak value, then dropping to a lower value before finally rising rapidly. These profiles give average peak and breakthrough torque values of 0.30 and 0.23 N m respectively.

The theoretical torque profile corresponding to experiment 1 (Fig. 6) is superimposed on the experimental curves in Figs 8a and b. Also, the experimental curve with the worst maximum error is filtered and shown in Fig. 9, together with the corresponding original and theoretical curves. The root mean square (r.m.s.) error between the experimental and theoretical curves for the filtered and original signals is 0.055 and 0.072 N m respectively. It can be seen that there is good

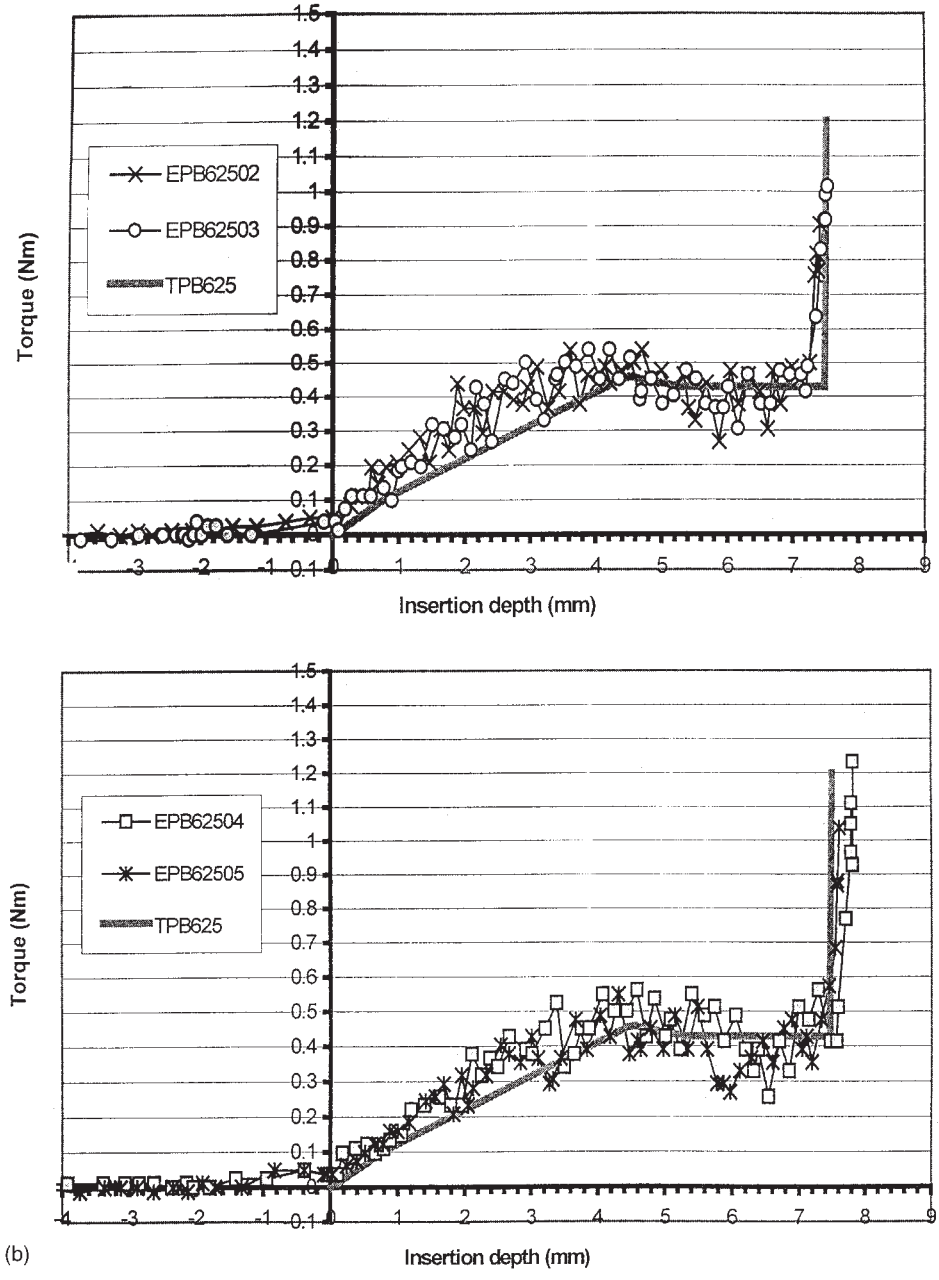

Fig. 8 Experimental torque profiles for four insertions on ABS plastic using screw AB 6 and the corresponding theoretical torque profile: (a) test 1a; (b) test 1b

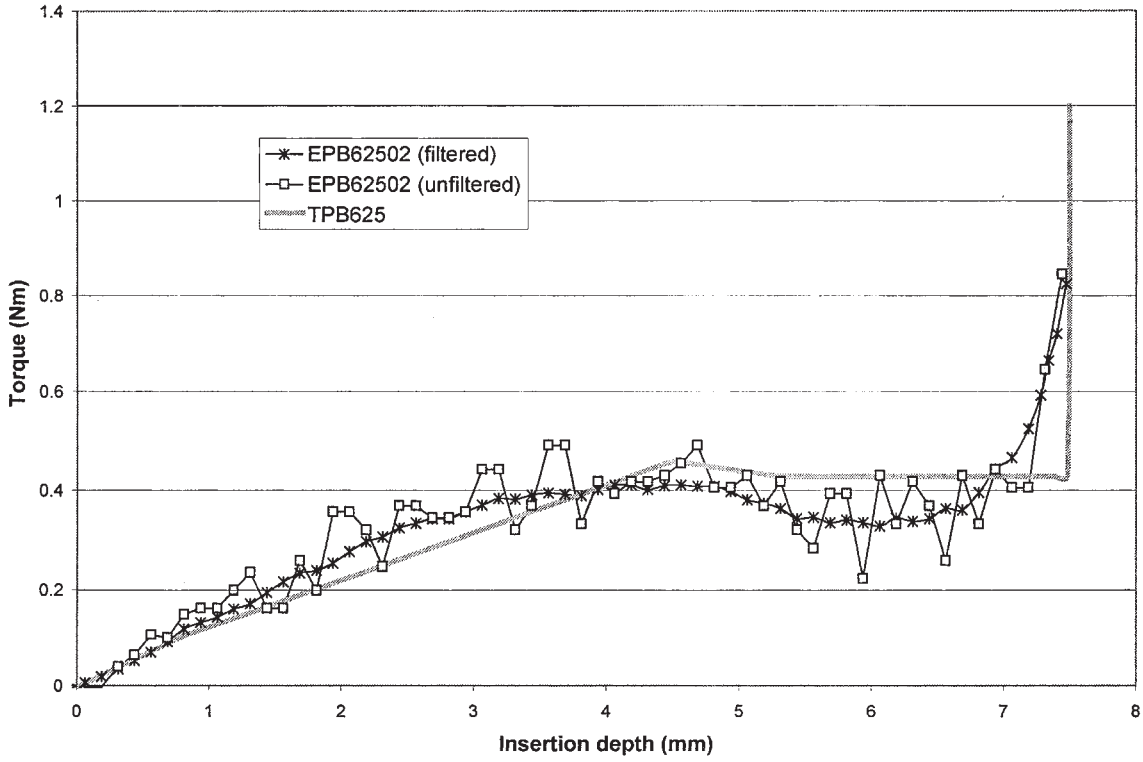

Fig. 9 Filtered and unfiltered torque profiles for one insertion on ABS plastic using screw 6 (EPB65202) and the corresponding theoretical profile

agreement between the theoretical curves and the experimental results.

7.2 Experiment 2—Insertion results for polycarbonate

Figures 10a and b show the insertion torque profiles for the experiment with the polycarbonate plate. In general, the shape of the torque profiles is the same as in the previous experiment 1, but the drop in torque from peak is more substantial than for ABS, reflecting the higher ultimate strength against the smaller plate thickness.

The theoretical torque profile corresponding to experiment 2 (Fig. 7) is superimposed on the experimental curves in Fig. 10. Also, the experimental curve with the worst maximum error is filtered and shown in Fig. 11, together with the corresponding original and theoretical curves. The r.m.s. error between the experimental and theoretical curves for the filtered and original signals is 0.050 and 0.068 N m respectively. Again, it can be seen that there is good agreement between the theoretical curves and the experimental results.

8 CONCLUSIONS

A theoretical model for the screw insertion process is presented, considering an ideal, general self-tapping screw insertion operation. When the screw is inserted, it will first advance, cutting a helical groove in the hole walls while overcoming friction. Then, an appropriate tightening torque is applied when the screw head makes contact with the top plate.

The screw insertion process is considered in three distinct phases: engagement, advancement and tightening. It is noted that, when the screw length is greater than the tap-plate thickness, the advancement phase has three distinct stages. Thus, a general self-tapping screw insertion process consists of five distinct stages. For each of the above phases, a quasi-static analysis was performed. The forces acting on the screw were examined using stress analysis concepts, and torque equations were derived for each stage, considering equilibrium conditions. The torque–displacement curve depends on the screw and plate parameters and material properties.

The theoretical model is used to generate torque–displacement curves for two examples employing ABS and polycarbonate plate materials and screw types AB 6 and 4 respectively. These curves are compared with corresponding experimental results, indicating good agreement.

In order to improve predictive accuracy, further factors such as lubrication, insertion axial forces, variation in material properties with temperature and lower plate-hole diameters larger than the root diameter of the screws need to be considered in future work.

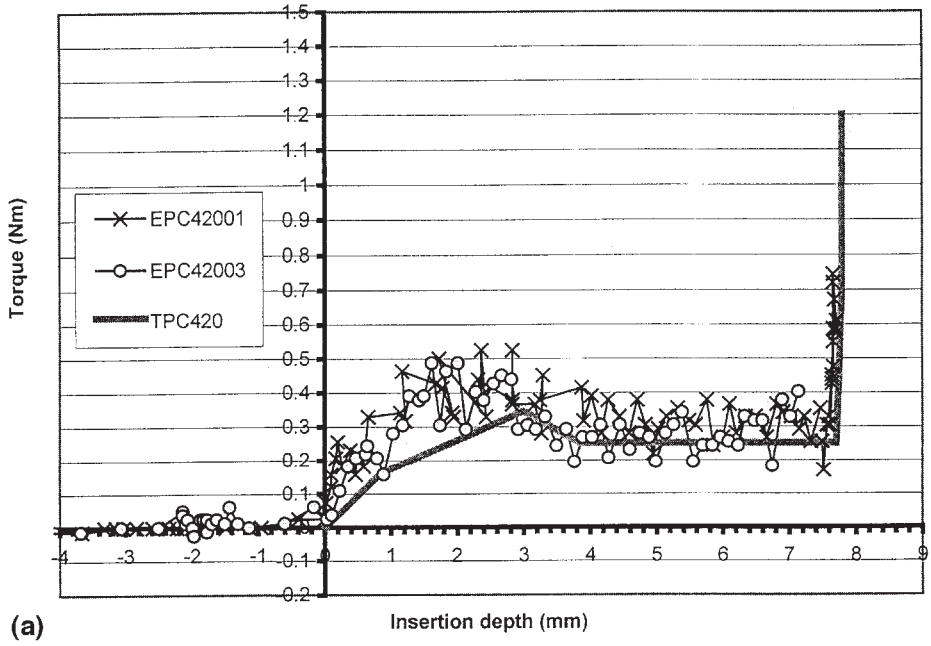

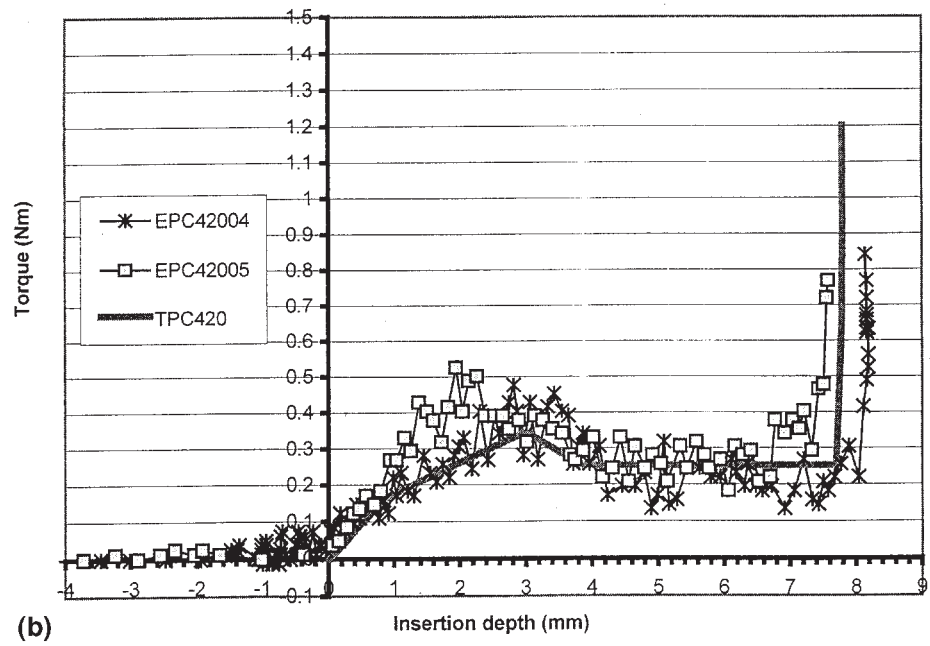

Fig. 10 Experimental torque profiles for four insertions on polycarbonate using screw AB 4 and the corresponding theoretical torque profile: (a) test 2a; (b) test 2b

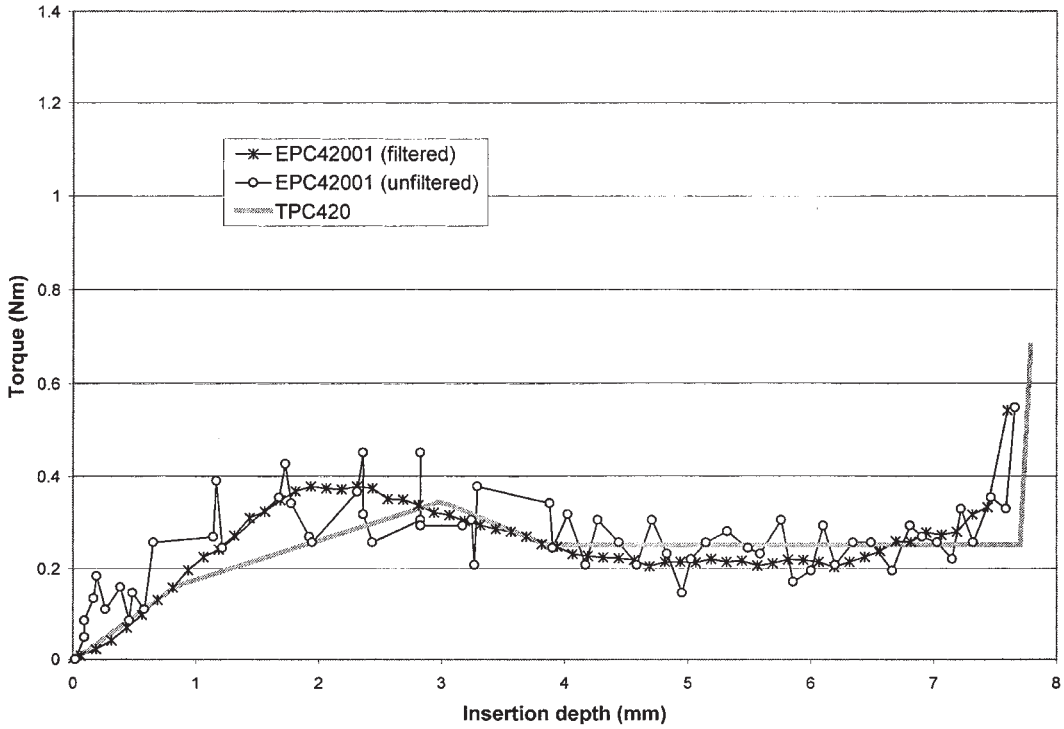

Fig. 11 Filtered and unfiltered torque profiles for one insertion on ABS plastic using screw 6 (EPB65202) and the corresponding theoretical profile

The present analysis of the self-tapping screw insertion process can be used to predict the expected axial torque. This model can be used for simulating the screw insertion process and for developing automated control and monitoring strategies.

REFERENCES

1 **Nevins, J. L.** and **Whitney, D. E.** Computer-controlled assembly. *Scient. Am.*, 1978, **238**(2), 62–74.
2 **Kondoleon, A. S.** Application of technology-economic model of assembly techniques to programmable assembly machine configuration. SM thesis, Mechanical Engineering Department, Massachusetts Institute of Technology, May 1976.
3 **Smith, S. K.** Use of a microprocessor in the control and monitoring of air tools while tightening threaded fasteners. *Proc. Soc. Mfg Engrs*, 1980, **2**, 397–421 (Dearborn, Michigan).
4 **Ogiso, K.** and **Watanabe, M.** Increase of reliability in screw tightening. In Proceedings of 4th International Conference on *Assembly Automation*, Tokyo, Japan, October 1982, pp. 292–302.
5 **Nicolson, E. J.** and **Fearing, R. S.** Compliant control of threaded fastener insertion. *IEEE J. Robotics and Automn*, 1993, 484–490.
6 **Seneviratne, L. D., Ngemoh, F. A.** and **Earles, S. W. E.** An experimental investigation of torque signature signals for self-tapping screws. *Proc. Instn Mech. Engrs, Part C, Journal of Mechanical Engineering Science*, 2000, **214**(C2), 399–410.

APPENDIX 1

Torque required to displace material

When the cutting portion of the screw thread advances along the helix by an elemental increment represented by $\delta\phi$, a force δF_s will have to be exerted normally on an elemental area of the plate material, δA, on the plane of the thread cross-section at that point (Fig. 4b). From stress theory and considering the maximum shear stress yield criteria, the resulting maximum shear stress acts on a plane that is at an angle of 45° to the screw thread minimum section area plane. The shear force on this plane, resulting from δF_s, is given by $\delta F_s \sin 45°$, and the area on which it acts is $\delta A / \cos 45°$. The shear stress on this plane is thus given by

$$\tau_{max} = \delta F_s \sin(\pi/4) \cos(\pi/4)/\delta A = \delta F_s/2\delta A$$

The maximum shear stress τ_{max} can be approximated to $\sigma_{max}/2$, where σ_{max} is the maximum compressive stress required to fracture the plate material under uniaxial loading. For engineering purposes and as a first approximation, it is assumed that $\sigma_{max} = \sigma_{uts}$, the ultimate tensile strength of the tap-plate material. Thus, the magnitude of the force vector is given by $\delta F_s = 2\tau_{max}\delta A = \sigma_{uts}\delta A$.

This force acts at the centroid of the elemental area δA, tangential to the groove helix, and moves with the screw thread along the helical path. Using the equation of the unit vector tangential to the helix, the elemental

force vector, $\delta \boldsymbol{F}_s$, at the groove helix coordinate position, ϕ, is given by

$$\delta \boldsymbol{F}_s \sigma_{uts}(-\cos\theta \sin\phi \boldsymbol{i} + \cos\theta \cos\phi \boldsymbol{j} + \sin\theta \boldsymbol{k})\delta A \quad (1)$$

where θ is the helix angle and is constant. For a linearly tapering cutting portion from C_1 to C_2, where C_1 is in contact with an arbitrary point on the groove with coordinate ϕ, and C_2 is in contact at coordinate ϕ–α on the groove, then

$$\frac{dA}{d\phi} = \frac{A_c}{\alpha} \quad (2)$$

along the *cutting portion* (it is noted that both α and ϕ are negative as they correspond to clockwise rotations), where A_c is the full-thread cross-sectional area on a plane normal to a tangent to the thread helix, and is given by $A_c = \frac{1}{2}ph$ when $D_h = D_r$. More generally, for any screw and hole combination where $D_s \geqslant D_h \geqslant D_r$

$$A_c = \tfrac{1}{4}(D_s - D_h)^2 \tan\beta \quad (3)$$

where β is the screw thread crest half-angle, and is constant. Substituting for δA in equation (1) gives

$$\delta \boldsymbol{F}_s = \frac{A_c \sigma_{uts}}{\alpha}(-\cos\theta \sin\phi \boldsymbol{i} + \cos\theta \cos\phi \boldsymbol{j} + \sin\theta \boldsymbol{k})\,\delta\phi \quad (4)$$

The elemental force vector $\delta \boldsymbol{F}_s$ generates a moment, $\delta \boldsymbol{M}_s$, about the fixed origin, O, at the top centre of the tap hole, given by the following cross-product:

$$\delta \boldsymbol{M}_s = \boldsymbol{R}_s \times \delta \boldsymbol{F}_s \quad (5)$$

where $\boldsymbol{R}_s$ is the position vector from the origin at the top centre of the tap hole to the point of action of $\delta \boldsymbol{F}_s$ on the *cutting portion* of the screw thread and is given by

$$\boldsymbol{R}_s = r_s \cos\phi \boldsymbol{i} + r_s \sin\phi \boldsymbol{j} + \frac{p}{2\pi}\phi \boldsymbol{k} \quad (6)$$

where r_s is the normal distance from the centre of the screw to the centroid of δA, the point of action of the elemental force vector, $\delta \boldsymbol{F}_s$. For the linear taper assumed, the mean value of r_s over the cutting portion applies and is equal to the normal distance from the screw centre to the centroid of the screw thread cross-sectional area.

From equations (4) to (6), the elemental torque, $\delta \boldsymbol{M}_{sz}$, about the screw central axis is given by

$$\delta \boldsymbol{M}_{sz} = \frac{A_c \sigma_{uts}}{\alpha}\left(r_s \cos\theta \cos^2\phi + r_s \cos\theta \sin^2\phi\right)\delta\phi \quad (7)$$

$\delta \boldsymbol{M}_{sz}$ being the resisting moment exerted by the sheared material on the screw thread element. Thus, to drive the element forward (not including friction), the applied torque, δT_{sz} must be in equilibrium with this shear resistance. Assuming quasi-static conditions, and considering the limit when $\delta\phi \to 0$, the elemental reaction torque about the screw central axis required to counteract $\delta \boldsymbol{M}_{sz}$ is given by

$$dT_{sz} = \frac{A_c \sigma_{uts}}{\alpha}\left(r_s \cos\theta \cos^2\phi + r_s \cos\theta \sin^2\phi\right)d\phi \quad (8)$$

At screw engagement and after screw breakthrough, the *cutting portion* is only partially engaged. To account for these situations, two discontinuous functions, ζ and ψ, are introduced for the lower and upper limits of integration respectively:

$$\zeta = 0 \qquad (0 \leqslant \phi \leqslant \alpha) \quad (9a)$$

$$\zeta = \phi - \alpha \qquad (\alpha \leqslant \phi \leqslant \phi_b + \alpha) \quad (9b)$$

$$\zeta = \phi_b \qquad (\phi \geqslant \phi_b + \alpha) \quad (9c)$$

$$\psi = 0 \qquad (\phi \leqslant 0) \quad (9d)$$

$$\psi = \phi \qquad (0 \leqslant \phi \leqslant \phi_b) \quad (9e)$$

$$\psi = \phi_b \qquad (\phi \geqslant \phi_b) \quad (9f)$$

where ϕ_b is the helix coordinate corresponding to the point where C_1 just emerges through the tap hole, i.e. the beginning of the screw breakthrough. The general equation for the axial cutting torque vector is then obtained by integrating equation (8) and employing the above limits, ζ and ψ:

$$T_{sz} = \frac{1}{\alpha} r_s A_c \sigma_{uts}[\psi(\phi, \alpha) - \zeta(\phi, \alpha)] \cos\theta \quad (10)$$

APPENDIX 2

Torque required to overcome friction

Considering an elemental screw thread surface of length δl, in contact with the groove surface at the helix coordinate position ϕ, a force, δF_{NO}, resulting from this interface pressure acts on the elemental surface, normal to its surface plane. The corresponding friction force, $\mu\delta F_{NO}$, acts along the surface plane in opposition to the motion of this element.

A triangular thread is considered, with the surfaces inclined to a normal to the helix by angle β (Fig. 2c). Let the normal forces on the lower and upper surfaces of the thread element be δF_{Nl} and δF_{Nu} respectively. As a result, friction forces $\mu\delta F_{Nl}$ and $\mu\delta F_{Nu}$ exist respectively on the lower and upper surfaces of the element (Fig. 12a). To facilitate the visualization of the components of these forces, a local cylindrical coordinate system $[\boldsymbol{n}, \boldsymbol{t}, \boldsymbol{z}]$ (Fig. 3c) is introduced, with the origin at the centre of the element, O', the $\boldsymbol{n}$ and $\boldsymbol{t}$ axes normal and tangential to the screw cylinder, respectively, and the $\boldsymbol{z}$ axis parallel to the screw central axis. The normal and friction forces on the element can be resolved into three mutually

perpendicular components δF_{fn}, δF_{ft} and δF_{fz}, in $[\boldsymbol{n}, \boldsymbol{t}, \boldsymbol{z}]$ directions as follows:

$$\begin{aligned}
\delta F_{fn} &= -\delta F_{Nu} \sin\beta - \delta F_{Nl} \sin\beta \\
\delta F_{ft} &= -\delta F_{Nu} \cos\beta \sin\theta + \delta F_{Nl} \cos\beta \sin\theta \\
&\quad + \mu\delta F_{Nu} \cos\theta + \mu\delta F_{Nl} \cos\theta \\
\delta F_{fz} &= -\delta F_{Nu} \cos\beta \cos\theta + \delta F_{Nl} \cos\beta \cos\theta \\
&\quad + \mu\delta F_{Nu} \sin\theta + \mu\delta F_{Nl} \sin\theta
\end{aligned}$$

These can be generally expressed in matrix notation as

$$\begin{bmatrix} \delta F_{fn} \\ \delta F_{ft} \\ \delta F_{fz} \end{bmatrix} = \begin{bmatrix} -\sin\beta & -\sin\beta & 0 & 0 \\ -\cos\beta\sin\theta & \cos\beta\sin\theta & \cos\theta & \cos\theta \\ -\cos\beta\cos\theta & \cos\beta\cos\theta & \sin\theta & \sin\theta \end{bmatrix} \times \begin{bmatrix} \delta F_{Nu} \\ \delta F_{Nl} \\ \mu\delta F_{Nu} \\ \mu\delta F_{Nl} \end{bmatrix} \tag{11}$$

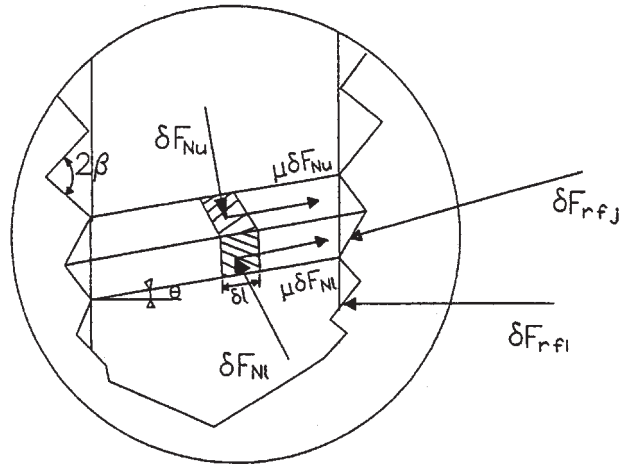

(a) Friction forces on screw thread

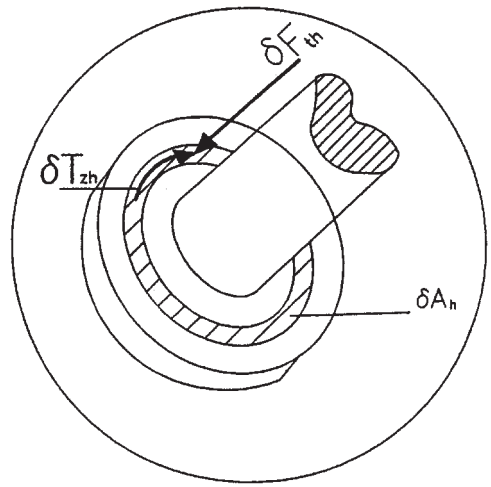

(b) Tightening forces on screw cap
$-T_h$, F_h

Fig. 12 Forces on screw

The coordinate system $[\boldsymbol{n}, \boldsymbol{t}, \boldsymbol{z}]$ rotates with the thread element as the screw advances. It can be transformed on to a fixed coordinate system $[\boldsymbol{x}, \boldsymbol{y}, \boldsymbol{z}]$, at the top centre of the tap hole using the transformation matrix $\mathbf{C}_\mathrm{f}$ given by

$$\mathbf{C}_\mathrm{f} = \begin{bmatrix} \cos\phi & -\sin\phi & 0 \\ \sin\phi & \cos\phi & 0 \\ 0 & 0 & 1 \end{bmatrix}$$

Hence, the vector sum of the normal and friction forces, $\delta\boldsymbol{F}_\mathrm{f}$, is given by

$$\begin{bmatrix} \delta F_{\mathrm{f}i} \\ \delta F_{\mathrm{f}j} \\ \delta F_{\mathrm{f}k} \end{bmatrix} = \begin{bmatrix} \cos\phi & -\sin\phi & 0 \\ \sin\phi & \cos\phi & 0 \\ 0 & 0 & 1 \end{bmatrix} \times \begin{bmatrix} -\sin\beta & -\sin\beta & 0 & 0 \\ -\cos\beta\sin\theta & \cos\beta\sin\theta & \cos\theta & \cos\theta \\ -\cos\beta\cos\theta & \cos\beta\cos\theta & \sin\theta & \sin\theta \end{bmatrix} \times \begin{bmatrix} \delta F_{\mathrm{Nu}} \\ \delta F_{\mathrm{Nl}} \\ \mu\delta F_{\mathrm{Nu}} \\ \mu\delta F_{\mathrm{Nl}} \end{bmatrix}$$

Assuming that the axial force applied on the screw is just sufficient to counter the axial component of the resisting force, then, with symmetrical thread surfaces, $\delta F_{\mathrm{Nu}} = \delta F_{\mathrm{Nl}} = \delta F_{\mathrm{NO}}$. The above equation then reduces to

$$\delta\boldsymbol{F}_\mathrm{f} = \begin{bmatrix} \delta F_{\mathrm{f}i} \\ \delta F_{\mathrm{f}j} \\ \delta F_{\mathrm{f}k} \end{bmatrix} = 2\begin{bmatrix} -\sin\beta\cos\phi - \mu\cos\theta\sin\phi \\ -\sin\beta\sin\phi + \mu\cos\theta\cos\phi \\ \mu\sin\theta \end{bmatrix}\delta F_{\mathrm{NO}} \qquad (12)$$

As indicated above, δF_{NO} is the force arising from the stress, σ_f, acting on the elemental surface area, δA_f, of the engaged screw thread. On a full thread, the element has a length δl and width w (Fig. 2c) and

$$\delta F_{\mathrm{NO}} = \sigma_\mathrm{f}\delta A_\mathrm{f} = \sigma_\mathrm{f} w\,\delta l \qquad (13)$$

Length δl can be expressed in terms of the helix coordinate position, ϕ, as follows:

$$\delta l = \sqrt{r_\mathrm{f}^2 + \left(\frac{p}{2\pi}\right)^2}\,\delta\phi \qquad (14)$$

where r_f is the normal distance from the centre of the screw to the centre of the thread cross-sectional area P_l and p is the screw pitch.

For the particular thread geometry considered, w can be expressed as follows:

$$w = \tfrac{1}{2}(D_\mathrm{s} - D_\mathrm{h})\sqrt{1 + \left(\frac{p}{D_\mathrm{s} - D_\mathrm{r}}\right)^2} \qquad \text{for } D_\mathrm{h} \geqslant D_\mathrm{r}$$

Usually, the roots of the threads are at a diameter greater than the effective root diameter, D_{re}. For triangular thread profiles with crest angles 2β, the effective root diameter is given by $D_{\mathrm{re}} = D_\mathrm{s} - p/\tan\beta$. Hence, the general expression for w, for any triangular thread geometry, is given by substituting for D_r in the above equation:

$$w = \tfrac{1}{2}(D_\mathrm{s} - D_\mathrm{h})\sqrt{1 + \tan^2\beta} \qquad (15)$$

The mean radial distance, r_f, from the screw central axis to the point of action of the friction force is given by

$$r_\mathrm{f} = (D_\mathrm{s} + D_\mathrm{h})/4$$

Substituting for w and δl in equation (13) gives

$$\delta F_{\mathrm{NO}} = \tfrac{1}{2}\sigma_\mathrm{f}(D_\mathrm{s} - D_\mathrm{h}) \times \sqrt{(1 + \tan^2\beta)\left[\left(\frac{D_\mathrm{s} + D_\mathrm{h}}{4}\right)^2 + \left(\frac{p}{2\pi}\right)^2\right]}\,\delta\phi \qquad (16)$$

or

$$\delta F_{\mathrm{NO}} = \sigma_\mathrm{f} K_\mathrm{f}\delta\phi \qquad (17)$$

where K_f is a function of screw and hole parameters given by

$$K_\mathrm{f} = K_{\mathrm{f0}} = \frac{1}{2}(D_\mathrm{s} - D_\mathrm{h}) \times \sqrt{(1 + \tan^2\beta)\left[\left(\frac{D_\mathrm{s} + D_\mathrm{h}}{4}\right)^2 + \left(\frac{p}{2\pi}\right)^2\right]} \qquad (18)$$

Substituting equation (17) in equation (12) gives

$$\delta\boldsymbol{F}_\mathrm{f} = 2K_\mathrm{f}\sigma_\mathrm{f}\begin{bmatrix} -\sin\beta\cos\phi - \mu\cos\theta\sin\phi \\ -\sin\beta\sin\phi + \mu\cos\theta\cos\phi \\ \mu\sin\theta \end{bmatrix}^{\mathrm{T}}\begin{bmatrix} \boldsymbol{i} \\ \boldsymbol{j} \\ \boldsymbol{k} \end{bmatrix}\delta\phi \qquad (19)$$

The elemental force vector, $\delta\boldsymbol{F}_\mathrm{f}$, acts through the centre of the elemental thread surface δA_f whose position, $\boldsymbol{R}_\mathrm{f}$, is given by

$$\boldsymbol{R}_\mathrm{f} = r_\mathrm{f}\cos\phi\boldsymbol{i} + r_\mathrm{f}\sin\phi\boldsymbol{j} + \frac{p}{2\pi}\phi\boldsymbol{k} \qquad (20)$$

Hence, the moment of $\delta \boldsymbol{F}_f$ about the origin is given by the vector product of equations (20) and (19):

$$\delta \boldsymbol{M}_f = \boldsymbol{R}_f \times \delta \boldsymbol{F}_f \tag{21}$$

Assuming quasi-static conditions, and considering the limit when $\delta\phi \to 0$, the elemental reaction torque about the screw central axis required to counteract δM_{fz} is given by

$$[\mathrm{d}T_{fz}] = 2K_f\sigma_f[r_f\mu \cos\theta]\,\mathrm{d}\phi \tag{22}$$

The reaction torque about the screw central axis, required to overcome friction resistance, can be obtained from equation (22) by integrating over the engaged thread surface. This consists of two parts:

1. Integration over the surface of full threads, where the crest of the threads are at a diameter equal to the major diameter of the main screw body. Since w is constant, K_f is also constant. The limits of integration are α and $\min(\phi - \alpha, \phi_b)$.
2. Integration over the surface of the cutting portion, defined by the helical displacement angle, α, where the crest of the threads are at diameters that progressively vary from the minor to the major diameter of the main screw body. As such, $K_f = K_f(\phi)$. For a linearly tapering cutting portion, the value of K_f associated with each element of the screw thread entering the hole, corresponding to $\delta\phi$, can be represented by the variation shown in Fig. 13a. Integration of any function of the form $CK_f(\phi)\,\mathrm{d}\phi$ is equal to C multiplied by the area under the curve of $K_f(\phi)$.

Let the area under the curve up to the coordinate position ϕ be represented by the function

$$Y(\phi) = \int_0^{\phi} CK_f\,\mathrm{d}\phi \tag{23}$$

The object is to find a good approximation for K_f that makes Y a linear function of ϕ. Such a function would be easier to handle for control purposes. Figure 13b shows a possible approximation function for K_f. Using this function, the corresponding area under the curve is given by

$$\begin{aligned} Y_1 &= \int_0^{\phi} CX_1\,\mathrm{d}\phi \\ &= \int_{\alpha/2}^{\min[\phi,\phi_b+(\alpha/2)]} CK_{f0}\,\mathrm{d}\phi \\ &= CK_{f0}\,\min\left(\phi - \frac{\alpha}{2}, \phi_b\right) \end{aligned} \tag{24}$$

From Fig. 13 and equation (24), the function Y_1 can be compared with the function Y:

$$Y_1 = Y \qquad \text{for } (\alpha < \phi < \phi_b)$$

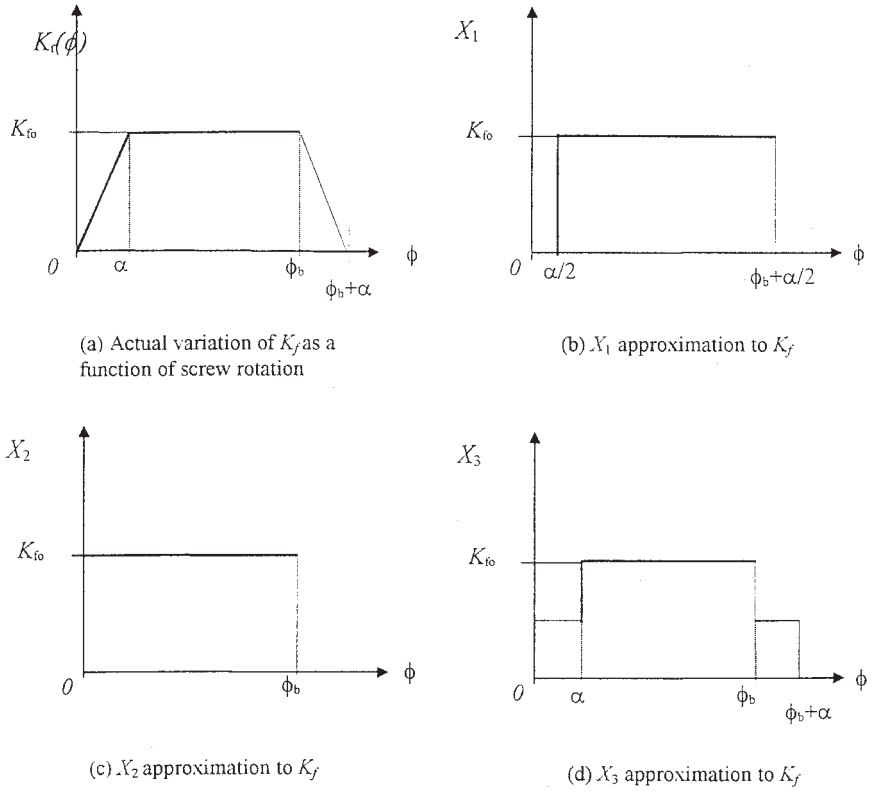

(a) Actual variation of K_f as a function of screw rotation

(b) X_1 approximation to K_f

(c) X_2 approximation to K_f

(d) X_3 approximation to K_f

Fig. 13 Different approximation functions to the thread friction area parameter K_f

and

$$\phi > \phi_b + \alpha;\ \text{maximum deviation } Y_1 - Y = -CK_{f0}\,\alpha/2$$

The torque component, T_{fz}, required about the screw central axis to counter friction resistance is obtained from equation (22) and given by

$$T_{fz} = 2\int_{\alpha/2}^{\phi} \mu r_f K_{f0}\sigma_f \cos\theta\, d\phi = 2\mu r_f K_{f0}\sigma_f \cos\theta\left(\phi - \frac{\alpha}{2}\right) \quad (25)$$

In the above integrals the use of ϕ for the upper limit of integration is valid only for the range $(\alpha/2) \leqslant \phi \leqslant \phi_b + (\alpha/2)$, where ϕ_b is the screw rotation angle at breakthrough. When $\phi > \phi_b + (\alpha/2)$, ϕ is substituted with $\phi = \phi_b + (\alpha/2)$. Hence, the axial torque component can be generally expressed as

$$T_{fz} = 2\mu r_f K_{f0}\sigma_f \cos\theta \min\left[\left(\phi - \frac{\alpha}{2}\right), \phi_b\right] \quad (26)$$

APPENDIX 3

Torque required to engage the screw

Consider a screw thread element in contact with the hole wall at an axial position z, and angular displacement, Φ, with a force F_e, applied on the screw head. For equilibrium:

$$F_e = \sigma_1(z)\,\Delta A_e \quad (27)$$

where σ_1 is the stress in the hole wall resulting from the application of F_e and A_e is the contacting surface area on which σ_1 acts.

Consider the screw further subjected to a torque component, T_e, so that the screw thread element now rotates at an angular velocity Φ', in addition to any axial velocity z'. The thread element is at a diameter greater than the hole diameter, and, for this state of motion to be sustained, the following force components are needed:

1. Forces elastically to deform the hole wall as the element rotates in the hole. The axial force is given by

$$F_{es} = \sigma_2\,\Delta A\,\mathrm{cosec}(\theta - \theta_e) \quad (28)$$

where ΔA is the elemental thread area on the thread cross-sectional plane, and θ_e is the angle of the force vector to the screw horizontal plane given by

$$\tan\theta_e = \frac{z'}{2\pi r_e \Phi'} \quad (29)$$

The deformation force, δF_{es}, acts at a radial distance, r_e, to the screw central axis. The moment component about the screw central axis is hence given by

$$T_{es} = r_e\sigma_2\,\Delta A\,\mathrm{cosec}(\theta - \theta_e)\cos(\theta_e) \quad (30)$$

2. Forces to overcome friction resulting from the sliding of the thread surface in contact with the stressed hole wall are

$$F_{ef} = \mu\sigma_2\,\Delta A_f + \mu\sigma_1\,\Delta A_e \quad (31)$$

$$T_{ef} = \mu r_e \cos(\theta_e)[\sigma_2\,\Delta A_f + \sigma_1\,\Delta A_e] \quad (32)$$

The applied axial torque equilibrium becomes

$$T_e = T_{es} + T_{ef}$$

$$T_e = r_e\sigma_2\,\Delta A\,\mathrm{cosec}(\theta - \theta_e)\cos(\theta_e) + \mu r_e\cos(\theta_e)[\sigma_2\,\Delta A_f + \sigma_1\,\Delta A_e] \quad (33)$$

Depending on the applied force and torque, the element of the screw thread may proceed along a helical path of angle θ_e, in the range $\theta \leqslant \theta_e \leqslant \pi/2$.

If $\theta_e = \theta$, the screw thread element advances along a helical path in the hole with the same helix angle as that on the screw. The screw is engaged when $dz/d\Phi = 2\pi r_e \tan\theta$.

The helix angle is given by $\tan\theta = p/2\pi r_e$, hence the condition for screw engagement is

$$\frac{dz}{d\Phi} = p \quad (34)$$

and equation (33) reduces to

$$T_e = r_e\cos\left(\frac{p}{2\pi r_e}\right)\sigma_2[\Delta A + \mu\,\Delta A_f] \quad (35)$$

The parameters ΔA and ΔA_f relate to the part of the thread cutting portion in contact with the groove at this point of engagement. If γ is the fraction of the cutting portion in contact with the groove, then the screw is engaged by $\gamma\alpha$ radians, and ΔA and ΔA_f can be expressed in terms of $\gamma\alpha$. Furthermore, since the stress component, σ_2, rises rapidly with the increasing groove on the hole wall, the material at this point will usually be at the point of permanent deformation, so that the torque required to engage the screw can be written as

$$T_e = r_e\cos\left(\frac{p}{2\pi r_e}\right)\sigma_y[\gamma A_c + \mu K_f\gamma\alpha] \quad (36)$$

where σ_y is the yield strength of the plate material. The angle $\gamma\alpha$ corresponds to the helix angle, ϕ_e, through which the screw turns to be engaged, i.e. $\phi_e = \gamma\alpha$ and $\gamma = \phi_e/\alpha$. Also, the screw hole parameter, K_f, can be approximated as a linear function of ϕ over the engagement phase as shown in Fig. 13, so that

$K_f = (K_{f0}/\alpha)\phi$. Substituting for γ and K_f in equation (36) gives

$$T_e = r_e \cos\left(\frac{p}{2\pi r_e}\right)\sigma_y\left[\frac{A_c}{\alpha}\phi_e + \frac{\mu K_{f0}}{\alpha}\phi_e^2\right] \tag{37}$$

APPENDIX 4

Torque required to tighten the screw

The contact force, F_{th}, on the screw head during this final tightening is given by

$$F_{th} = \int \sigma_z \, dA_h \tag{38}$$

where σ_z is the compressive stress on the lower surface of the screw cap, and dA_h is an elemental area of the screw cap in contact with the plate. Assuming that the stresses are uniformly distributed gives

$$\sigma_z = Ee_z \tag{39}$$

where E is the elastic modulus of the plate material and e_z is the compressive elastic strain in the plate. Then equation (38) becomes

$$F_{th} = Ee_z A_h = \frac{\pi}{4} Ee_z(D_{sh}^2 - D_s^2) \tag{40}$$

The force on the screw cap is transmitted through the screw threads on to the formed threads on the tap plate, which in turn exerts an opposite reaction force on the screw threads, producing tension in the screw stem. The reaction force, F_{tb}, on the formed threads in the tap hole is equal to the screw head force, F_{th}, in the isolated case with no applied axial force. Force F_{tb} is distributed over the contact surface of the engaged threads, and, together with the force at the screw cap interface, produces both compression in the material as well as bending on the screw and hole threads.

The clamping force can be modelled as a pure compression force, F_{th}, acting on a cylinder with an outer diameter equal to the diameter of the screw head, an inner diameter equal to the screw diameter and a height equal to the sum of the near plate thickness, t_1, and the mean axial distance of engaged threads, z_{em} (Fig. 5).

When tightening occurs with the cutting portion of the screw thread still engaged in the hole ($t_1 + t_2 > L_s$), z_{em} is given by

$$z_{em} = p\phi_t/4\pi \tag{41a}$$

When tightening occurs with the cutting portion of the screw thread out of the tap hole, z_{em} is given by

$$z_{em} = t_2/2 \tag{41b}$$

Let the screw thread element move through an incremental angle $\Delta\phi$ after contact, so that the helix coordinate position is $\phi_t + \Delta\phi$. At the same time, the equivalent cylinder above will compress by Δt, while the screw and formed threads will deflect under the force F_{tb} by a total amount d, moving the screw in the opposite direction to the insertion direction, so that

$$\Delta t + d = p\,\Delta\phi/2\pi \tag{42}$$

The strain in the cylinder is then given by

$$e_z = \frac{\Delta t}{t_1 + z_{em}} = \frac{(p\,\Delta\phi/2\pi) - d}{t_1 + z_{em}} \tag{43}$$

Hence, the force on the screw cap is given by substituting equation (43) in equation (40):

$$F_{th} = \frac{\pi E(D_{sh}^2 - D_s^2)}{4(t_1 + z_{em})}\left(\frac{p\,\Delta\phi}{2\pi} - d\right)$$

$$= K_{th}\left(\frac{p\,\Delta\phi}{2\pi} - d\right) \tag{44}$$

where K_{th} is the equivalent axial spring stiffness coefficient of the parts sandwiched between the screw cap and the formed threads, given by

$$K_{th} = \frac{\pi E(D_{sh}^2 - D_s^2)}{4(t_1 + z_{em})} \tag{45}$$

As a result of the normal force, F_{th}, a friction torque is generated in reaction to any rotation of the screw head against the plate, given by

$$T_{th} = \int \mu_h \sigma_z r \, dA_h = \int_{R_1}^{R_2} 2\pi\mu_h\sigma_z r^2 \, dr \tag{46a}$$

where μ_h is the friction coefficient between the screw head and the near plate, $R_1 = D_s/2$ and $R_2 = D_{sh}/2$. If the stress is assumed to be uniformly distributed on the screw head and the friction coefficient is assumed to be constant over the friction surface, then equation (46a) becomes

$$T_{th} = \pi\mu_h\sigma_z(D_{sh}^3 - D_s^3)/12 \tag{46b}$$

Under a balanced axial force, the screwdriver is assumed to apply a sufficient axial force component to counteract the force on the screw head, F_{th}. In this respect, no additional force is set up in the screw stem as a result of F_{th} and, consequently, there is no upward deflection, d, of the screw threads. Force $F_{tb} = 0$ and, consequently, $T_{tb} = 0$. Hence, from equation (44), the driver axial force component, F_{tz}, against tightening resistance is given by

$$F_{tz} = -F_{th} = -K_{th}\left(\frac{p\,\Delta\phi}{2\pi}\right) \tag{47}$$

Substituting $\sigma_z = F_{th}/A_h$ in equation (46), the screw head torque component, T_{tz}, is given by

$$T_{tz} = \mu_h K_{th}\left(\frac{D_{sh}^3 - D_s^3}{3(D_{sh}^2 - D_s^2)}\right)\left(\frac{p\,\Delta\phi}{2\pi}\right) \tag{48}$$

T_{tz} is the axial torque required to tighten the screw, as a function of the screw rotation increment, to counter the resistance to the screw motion as a result of contact of the screw cap on the near plate surface.